COMPDYN 2013
4th ECCOMAS Thematic Conference on
Computational Methods in Structural Dynamics and Earthquake Engineering
M. Papadrakakis, V. Papadopoulos, V. Plevris (eds.)
Kos Island, Greece, 12–14 June 2013

SHAKE TABLE TESTING OF A FULL-SCALE FIVE-STORY BUILDING: SEISMIC PERFORMANCE OF PRECAST CONCRETE CLADDING PANELS

Elide Pantoli[1*], Michelle Chen[1], Tara Hutchinson[1], Glen A. Underwood[2], and Mark Hildebrand[3]

[1] University of California, San Diego, 9500 Gilman Drive, La Jolla, CA 92093-0085
elide.pantoli@yahoo.it; mchen.ucb@gmail.com; tara@ucsd.edu

[2] Clark Pacific, 1980 South River Road, West Sacramento, CA 95691
gunderwood@clarkpacific.com

[3] Willis Construction Co., Inc., 2261 San Juan Hwy, San Juan Bautista, CA 95045
mhildebrand@pre-cast.org

Keywords: Façades, Precast concrete cladding, shake table tests.

Abstract. *Precast concrete cladding (PCC) is used in many regions of the world as an architectural façade for buildings. Use of PCC is appealing in that panels can be constructed off-site and quickly installed on a finished structural skeleton to complete the building envelope. Detailing of the PCC panel joints and connections to the building must carefully consider the movement that the building will undergo during its service life – including the potentially intense effects of an earthquake. Although code prescribed seismic design requirements provide nominal guidance regarding the desirable features of the PCC and its connections, much is still unknown regarding their actual behavior during an earthquake. Moreover, to date, only a handful of full-scale tests have been conducted to investigate the behavior of the PCC under earthquake loading, and even fewer have been conducted with the PCC attached to a full-scale building.*

To address the need for system-level experimental data, a full-scale five-story building was tested on the Network for Earthquake Engineering Simulation (NEES) Large Outdoor High-Performance Shake Table at the University of California, San Diego. This structure was seismically tested in two phases, namely, while isolated and fixed at its base. Two different types of façades were installed on the building, namely a lightweight metal stud system overlaid with stucco and a punchout window-style PCC system. Push-pull, sliding, flexing, and a new yielding connection were investigated within the PCC system. In addition variation in the panel corner details were implemented. This paper describes the performance and the measured experimental response of the precast concrete cladding panels installed at the upper levels of the test building.

1 INTRODUCTION

Recent earthquakes have demonstrated that damage to nonstructural components and systems (NCSs) in buildings pose life safety hazards to the building occupants and lead to significant economic losses and repair downtime [1]. A particularly important and sensitive NCS is that which provides the exterior enclosure. Not only does this subsystem represent a significant portion of the cost of the building, varying between 9% and 18% of the total cost for different types of buildings [2], but exterior enclosures have also realized extensive damage in past earthquakes [3]. A prevalent type of façade commonly used worldwide is the precast concrete cladding (PCC) panelized system. In this type of façade, concrete panels are fabricated at a precast facility and brought to the site just prior to installation. They are attached to the building with steel connections that must provide a load path to the structure transferring not only their own weight, but also any lateral forces (wind/seismic) imposed on the panels. The connection system, however, must allow relative motion of the panel and structure due to the horizontal building displacements – both in-plane and out-of-plane – during seismic motions. Connections that hold the panels to the structure for out-of-plane forces while accommodating these *interstory drift* displacements are designated as *push-pull* or *tie-back* connections. In practice, two types of push-pull connections are used, namely, sliding connections and flexing rod connections. In both cases the out-of-plane force is resisted by the axial action of the rod. In a sliding connection, the panel is allowed to move in the in-plane direction via sliding of the connection rod in a slot. In contrast, a flexing rod connection allows movement through the bending of the connection rod. In either case, the sliding or bending capacity must be enough to allow the maximum interstory drift. The performance of the connections can vary considerably by changing the length (L) to diameter (Φ) ratio of the rods. For sliding rod connections, a longer rod may facilitate the installation of the panels, however, if the rod is too long it might not be stiff enough and may begin to yield under bending during a large earthquake. For the flexing rod connections, a shorter rod might not be able to provide enough ductility but a longer rod might occupy too much space. Another detail of critical importance for the performance of the PCC panels is the size of the panel-to-panel joints: the joints have to be big enough to avoid collision of the panels during earthquake motion. However, for aesthetic reasons, large joints are undesireable.

Historically, this construction method has performed well in past earthquakes – including the 1994 Northridge event, which resulted in large story drifts in buildings with limited damage to precast cladding systems [4]. Nonetheless, instances of damage to these panel systems have been reported in several earthquakes. Recently for example, during the Christchurch earthquake in 2011 in New Zealand several panels failed due to inadequate detailing. Moreover, extensive cracking, corner crushing, residual displacement of the panels and rupture of the seal at panel interfaces were reported [3]. During the Chile earthquake in 2010, several PCC panels collapsed in the out-of-plane direction. In one case, the cause of collapse was local bending failure of the flanges of an embedded anchor channel, which allowed pullout of the sliding bolt [5]. Several pullout failures of tie-back connections were also observed following the L'Aquila earthquake in Italy in 2006 [6]. Large scale testing of these PCCP, particularly if integrated within a building system would help understand their behavior. However, such testing is highly complex and costly, therefore to-date only a few full-scale experiments on these panels have been conducted [7,8].

1.1 Scope of this Paper

In April and May 2012, a landmark test of a five-story building constructed at full-scale and completely furnished with nonstructural components and systems (NCSs) was conducted

at the University of California, San Diego (UCSD) Network for Earthquake Engineering Simulation (NEES@UCSD, 2013) facility. The project, coined *Building Nonstructural Components and Systems (BNCS)* was realized by a unique collaboration between Academe, Industry and Government and hundreds of individuals with expertise in structural and nonstructural design, earthquake engineering, and construction and management practices (BNCS, 2013). The full-scale building-NCS system was seismically tested in a base isolated and fixed based configuration on the Large High-Performance Outdoor Shake Table (LPOSHT) at the UCSD-NEES facility. Wrapping the exterior of this building were two types of façades, namely; light weight metal stud balloon-framing overlaid with a synthetic stucco finish (first three floors) and precast concrete cladding panels (PCC panels) (two upper floors). This paper will describe the test parameters considered in the design of the PCC panels installed at the upper floors of the building, their instrumentation, the overall test protocol, and select physical and analog measured results specific to the PCC panels.

2 DESCRIPTION OF THE EXPERIMENT

The poured in place reinforced concrete five story building was fully equipped with a wide range of NCSs, including a fully functional passenger elevator, stairs, mechanical and electrical services, ceiling and piping subsystems, as well as roof mounted equipment. Different occupancy types were specified for each floor level within the building. The fourth and the fifth floor were equipped as medical floors (resembling an intensive care unit and a surgical suite, respectively). The overall height of the specimen, including its foundation, was 22.8m, its length was 11.5m and its width 7m. The bare structure had an estimated weight of 3010 kN, excluding the foundation which weighed 1870 kN. Including the NCSs, the building weighed approximately 4420 kN. The floor plan was characterized by the presence of two large openings (one for the stairs and one for the elevator) and two walls encasing the elevator shaft (Figure 1). It is important to underline that the LHPOST at NEES@UCSD allows movement only in the East-West direction (longitudinal direction of the building). Two bays in the longitudinal (shaking) direction and one bay in the transverse direction provided the load bearing system. Lateral seismic resistance was provided by a pair of identical one-bay special moment resisting frames in the Northeast and Southeast bays.

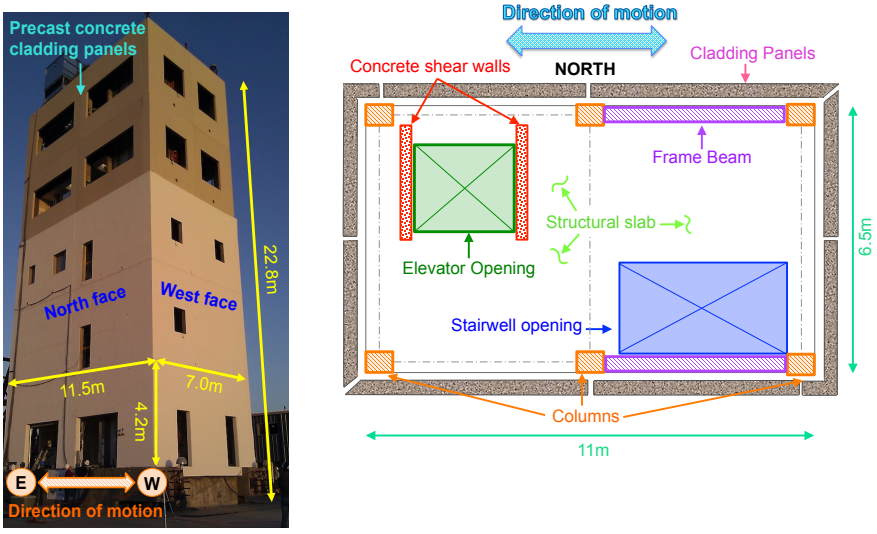

(a) (b)

Figure 1: General views of the test building: (a) photograph of the North and West sides of the building and (b) plan view of a typical floor

The building was initially tested while isolated from the shake table with four high damping rubber bearings installed between at each of the four corners of the structure. Following the base isolation (BI) test phase, the foundation was fixed to the table and the building was then tested with a fixed base configuration (FB). The building was subjected to a suite of earthquake motions of increasing intensity: seven motions were used while in the BI configuration and six motions while in the FB configuration. In addition, white noise and pulse base excitation were input before and after earthquake motion input. Initial motions were selected and scaled to an intensity associated with a serviceability event. Motions from the Maule, Chile (2010) and the Pisco, Peru' (2007) earthquakes were chosen due to their inherently long duration of strong shaking. The latter record was also input into the model multiple times at increasing amplitudes. Two final motions were spectrally matched and scaled records obtained during the Denali earthquake in Alaska (2002). The goal of these motions was to reach and surpass the design level earthquake. The sequence of motions applied in the first portion of the BI test phase was repeated for a portion of the FB test phase. In some cases the actual motion (AM) was used as the target, while in other cases the original motion was spectrally matched (SM) to the ASCE 7-05 design spectrum assuming a high seismic zone in Southern California (site class D). The LAC motion was run twice in the BI configuration. The full test protocol is shown in Table 1.

Base	Station-scale (Earthquake)	Name	Type	Notes
Isolated (BI)	Canoga Park-100% (1994 Northridge earthquake)	BI-1: CNP100	SM	Serviceability level
	LA City Terrace-100% (1994 Northridge earthquake)	BI-2:LAC100	SM	Serviceability level
	LA City Terrace-100% (1994 Northridge earthquake)	BI-3:LAC100	SM	Serviceability level
	San Pedro-100% (2010 Maule-Chile earthquake)	BI-4:SP100	AM	Long duration
	ICA-50% (2007 Pisco-Peru earthquake)	BI-5:ICA50	AM	Long duration, multiple runs
	ICA-100% (2007 Pisco-Peru earthquake)	BI-6:ICA100	AM	Long duration, multiple runs
	ICA-140% (2007 Pisco-Peru earthquake)	BI-7:ICA140	AM	Long duration, multiple runs
Fixed (FB)	Canoga Park-100% (1994 Northridge earthquake)	FB-1:CNP100	SM	Serviceability level
	LA City Terrace-100% (1994 Northridge earthquake)	FB-2:LAC100	SM	Serviceability level
	ICA-50% (2007 Pisco-Peru earthquake)	FB-3:ICA50	AM	Long duration, multiple runs
	ICA-100% (2007 Pisco-Peru earthquake)	FB-4:ICA100	AM	Long duration, multiple runs
	Pump Station #9-67% (2002 Denali eq.)	FB-5:DEN67	SM	~Design Earthquake
	Pump Station #9-100% (2002 Denali eq.)	FB-6:DEN100	SM	~>50% larger than Design Earthquake

Table 1: Seismic test protocol (AM = actual motion as target; SM = spectrally matched motion as target).

3 DESCRIPTION OF THE PRECAST CONCRETE CLADDING PANELS

Through support of the Charles Pankow Foundation and an industry advisory board within the Precast Concrete Institute (PCI), a team of researchers and precast concrete producers worked closely on the design, construction, installation, and instrumentation of the precast concrete panels tested within the BNCS building specimen.

3.1 Overview

Panels selected for this test program were punched window wall units, meaning they spanned from floor to floor with openings provided only for windows. Two panels per side of the building were installed at each floor, resulting in a total of 16 panels mounted on the test building. Eight panels translate predominantly in the in-plane direction (denoted as *IP* panels) and eight panels tilt predominantly in the out-of-plane direction (denoted *OP* panels). Connection of the panels to the building skeleton were facilitated by steel embeds installed in the slab, beams and columns. Each panel was supported by two bearing connections at the bottom welded to embeds in the floor slab, and push-pull connections at the top (four in the IP panels and two in the OP panels). The IP panels had an average dimension of 5.4m x 4.4m and an average weight of 50 kN, while the OP panels were smaller, with an average dimension (not considering the return corner) of 3.4m x 4.4m and an average weight of 39 kN. All panels were 125 mm in thickness and generally reinforced with #4 bars at 305mm o/c spacing in both directions. Details of the panel geometry can be found in Figure 2. Nomenclature adopted in this paper to describe the various panels and connections is shown in Figure 3. Two different types of corner joints were tested, namely, miter joints and butt joints (Figure 4). Miter joints were installed in the South-West and North-East corners, while butt joints were installed on the North-West and South-East corner.

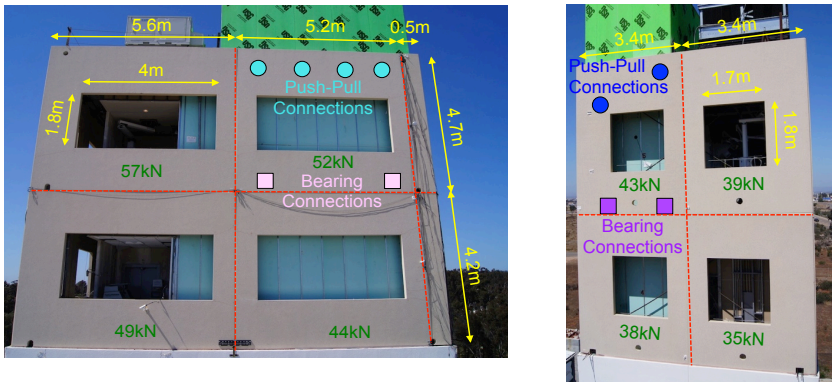

(a) (b)

Figure 2: View of the panels showing the geometry and the typical location of the connections: (a) IP panels on the South side and (b) OP panels on the East side

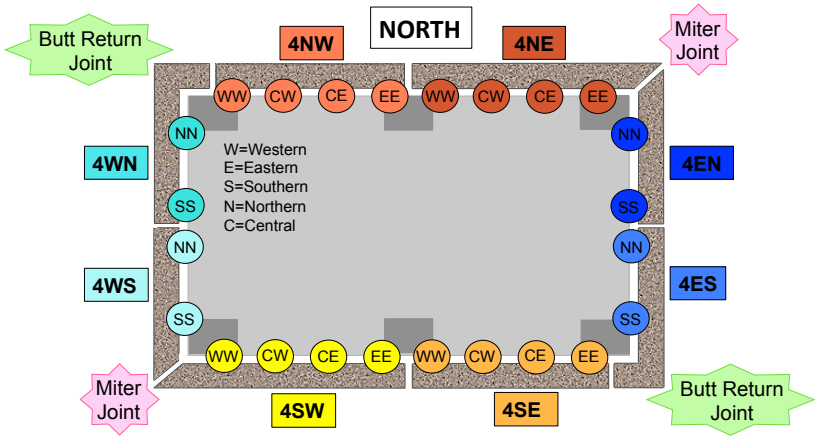

Figure 3: Nomenclature used to identify the panels and connections on the fourth floor. Nomenclature for the fifth floor panels are similar, with the exception that the first digit becomes "5".

(a) (b)

Figure 4: Corner joints: (a) miter joint in the SW corner and (b) butt return joint in the NW corner

3.2 Parameters of specific interest in the test program

The behavior of PCCP connections and panel joints was of paramount interest in this experiment because panel collisions and connection failures greatly affect whether panels become separated from a structure in a seismic event. Incidental damage and resulting affects on serviceability of the PCCP are also affected by panel joints and connectivity. For the IP panels, the main purpose of the connections is to absorb the relative drift from floor to floor, or interstory drift, while maintaining the ability to support the panel in the out-of-plane direction. This is commonly facilitated in practice via sliding or flexing rod connections (Figure 5), and is codified in United States practice within ASCE 7, Section 13.5.3 as follows [9]:

> ***13.5.3 Exterior Nonstructural Wall Elements and Connections***. *Exterior nonstructural wall panels or elements that are attached to or enclose the structure shall be designed to accommodate the seismic relative displacements defined in Section 13.3.2 and movements due to temperature changes. Such elements shall be supported by means of positive and direct structural supports or by mechanical fasteners in accordance with the following requirements:*

> *a. Connections and panel joints shall allow for the story drift caused by relative seismic displacements (D_p) determined in Section 13.3.2, or 0.5 in. (13mm), whichever is greatest.*
> *b. Connections to permit movement in the plane of the panel for story drift shall be sliding connections using slotted or oversize holes, connections that permit movement by bending of steel, or other connections that provide equivalent sliding or ductile capacity.*
> *c. The connecting member itself shall have sufficient ductility and rotation capacity to preclude fracture of the concrete or brittle failures at or near welds.*

These code provisions provide a good basis for design of cladding joints and connections, but still leave designers to their own devices when it comes to defining the meaning of qualitative terms like *"sufficient ductility and rotation capacity"*, especially considering the allowance of yielding in a connection to accommodate story drift displacements.

In the tested connections, the key variables for these mechanisms to work properly are the ratio of rod length to rod diameter (L/Φ), and the ratio of relative seismic displacements, D_p to rod length, L (D_p/L). It should also be noted that flexing rod connections need to be constructed of mild steel such as ASTM A36 or a ductile SAE range of ASTM A108 material to preclude a premature brittle fracture during cyclic bending. Sliding connections are often facilitated by a sliding rod and oversized hole in the support clip angle, with long plate washers either side to maintain contact (Figure 5a-b). Sliding connections can also be constructed with an embedded channel that allows the bolt to slide inside the channel on the panel side of the connection. This configuration was not tested. In general, a sliding connection works best when the surface with the slot is close to the surface that is sliding, i.e. when the rod is short. If the sliding rod is too long, bending and rotation of the rod will cause the connection to bind, leading to a shear failure of the rod. On the other hand, flexing rod connections benefit from longer rod lengths. The longer rod length helps reduce inelastic strains in the rod for a given displacement (Figure 5c-d). However, it should be noted that from a practical point of view, long rods may require too much space, infringing on interior finishes rather than being concealed in the perimeter framing spaces.

In these tests, several rod lengths were tested for each of the sliding and flexing rod connections, as summarized in Table 2. The diameter of the rods was 20mm for all IP panel connections. Pictures of a sliding connection with a long rod (SRL) and flexing rod connection with long rod (FRL) are provided in Figure 6. The IP panels on the West side of the building were installed with sliding rod connections, while those on the Eastern side were installed with flexing rod connections. The exact distribution of the upper connections in the panels is shown in Figure 7.

Type of connection	Short rod length (mm)	Short rod L/Φ	Medium rod length (mm)	Medium rod L/Φ	Long rod length (mm)	Long rod L/Φ
Sliding	snug	-	90	4.6	180	9.3
Flexing rod	300	16	405	21.3	510	26.6

Table 2: Summary of rod lengths tested

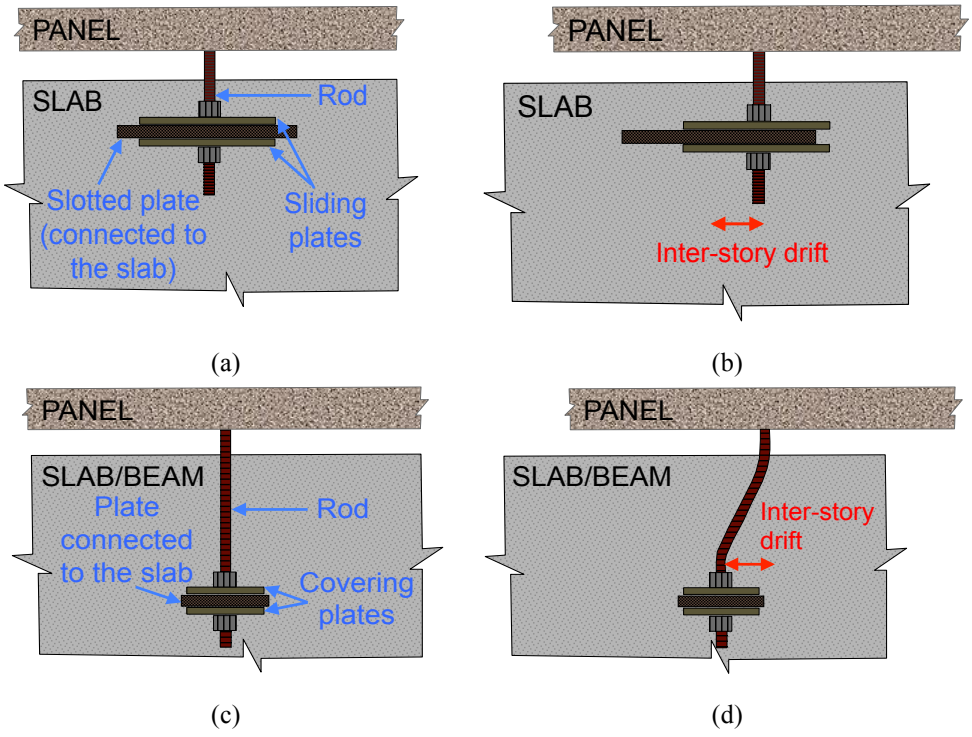

Figure 5: PCCP connections between structural skeleton and panel (schematic on left, desired behavior on right): (a), (b) sliding rod connection, and (c), (d) flexing rod connection.

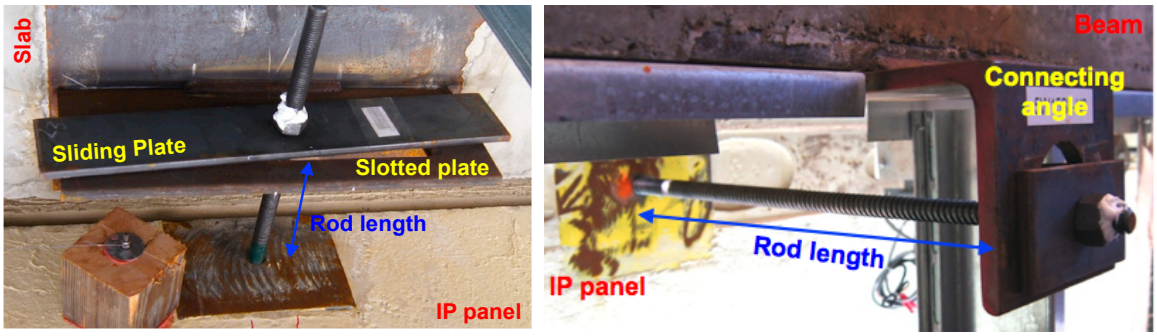

(a) (b)

Figure 6: Photographs of the connection details for the IP panels: (a), sliding rod connection with long rod and (b) flexing rod connection with long rod.

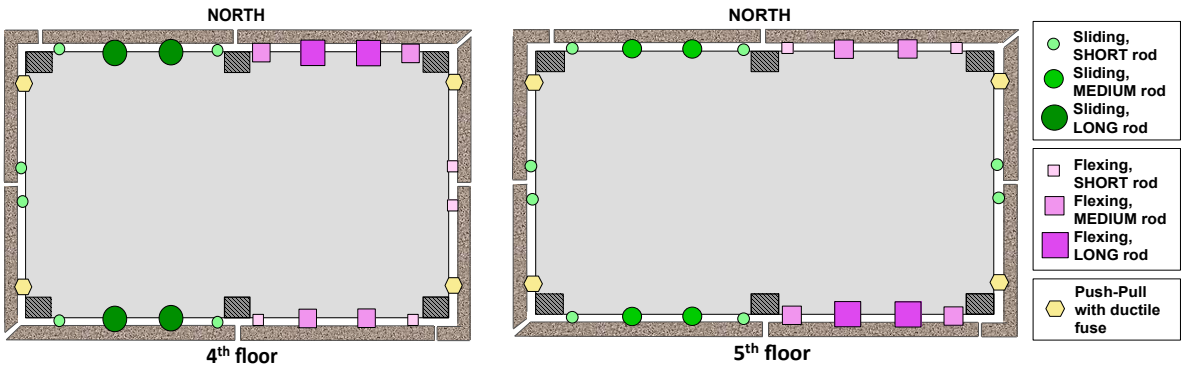

(a) (b)

Figure 7: Location of the different types of connections: (a) fourth floor and (b) fifth floor.

In addition to the traditional sliding and flexing connections, which are designed with the intent of allowing movement of the panels relative to the building, a new connection detail was explored. This detail would allow for smaller vertical joints between panels at the corners of the building, which is an architecturally appealing performance feature. This strategy was implemented within the OP panel connections at corner columns. Here, the width of vertical corner joints was intentionally undersized to 25mm (butt joint) and 19mm (miter joint). These joint sizes are intended to be sufficient to accommodate the elastic interstory drift of the structure without closing, but would not accommodate inelastic displacements that can be expected in the design basis earthquake (DBE). For this case, panel tilt (and joint closures) ranged on the order of 100mm for the most severe motions tested. Upon panel collision at the joint, the panel connection would activate a ductile fuse in the form of a cantilevered bending plate designed to yield as the structural column drifts along the shaking direction, while the panel motion is restrained by the contracted joint during contact (Figure 8). The ductility is provided by ensuring the expected plastic flexural capacity of the plate is less than the capacity of the welds, the rod in tension, and the concrete anchorages of the embeds in the column and the panel itself. For these connections, the rod was 700mm long, and the diameter was 25mm. Each of the OP panels had two push pull connections at the top of the panel, namely a corner push pull connection with ductile fuse (PPDF) as shown in Figure 8, and either a sliding rod connection with snug rod (SRS) or a flexing rod connection with short rod (FRS) connection (for the exact location see Figure 7).

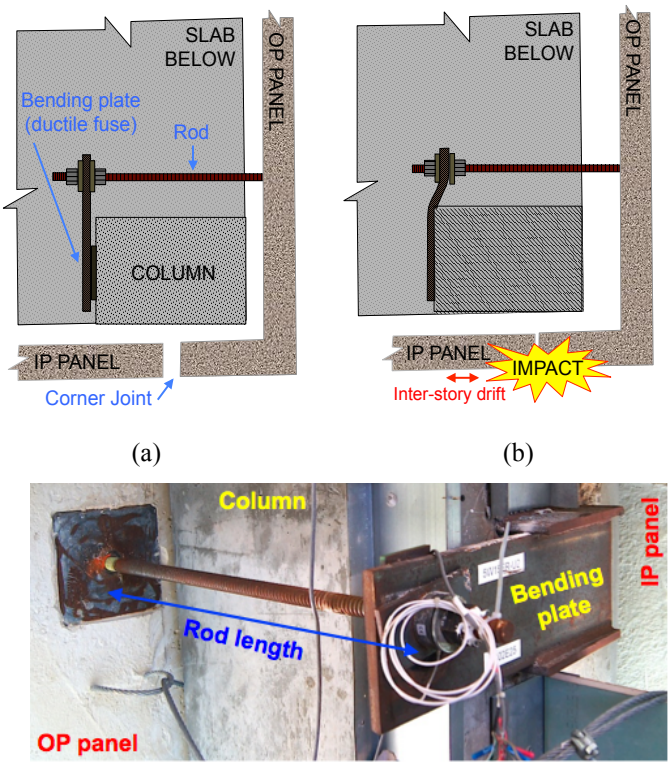

Figure 8: Push-pull connection with ductile fuse on the OP panels: (a), (b) drawings showing their desired behavior and (c) photograph.

3.3 Design, material properties and installation

Panel design, construction, and installation were performed by a U.S. West-Coast precaster with expertise in precast concrete cladding systems. Structural design criteria and detailing conformed to requirements of ASCE 7-05, ACI 318-08, PCI MNL 120-04 and ANSI/AISC 360-05 [9,10,11,12] for regions of high seismicity. Nonlinear time history analyses of the building were conducted and used to predict interstory drift ratios (IDRs) anticipated during design and maximum credible earthquake events [13] and thereby size the joints and design the slotted and flexing rod connections. Design forces were estimated using the building target S_{DS} and the linear force distribution estimate of ASCE 7 (equations 13.3-1). Panels were 127mm thick and reinforced with #4 bars A615 Grade 60 rebar spaced at 300mm on center. Additional #5 bars were added around window openings, and #3 horizontal bars at 150mm o/c were used in piers adjacent to windows. The specified compressive strength of concrete at 28 days was 34MPa with a unit weight of 2400 kg/m^3. Coil rods and bolts were ASTM A108 steel with yield and ultimate strengths of f_y = 410MPa and f_u = 550MPa, respectively.

Panels were cast off-site at a precast plant and shipped to the NEES@UCSD facility on the day of installation. In total, installation of the 16 panels on the building was performed during approximately five days, with the following activities:

- Day one: All connections were prepared, including welding of connection angles to the structural embeds cast in the building and placement of the rods;
- Day two and three: Eight panels per day were installed on the building; and
- Day four and five: Welding of all bearing connections at the base of the panels to the embeds in the structural slab and frame was complete.

Finally, several days were needed to place caulking between panel-to-panel joints and between the balloon framing-to-panel joints.

3.4 Instrumentation

A total of 65 analog sensors monitored the behavior of the cladding panels. The main goals were to monitor:

- The displacement at the top of the panel relative to the structural skeleton. In particular the in-plane movement of the IP panels and the out-of-plane movement of the OP panels were closely monitored;
- The acceleration in both IP and OP panels in order to understand a possible magnification of the acceleration in the panels. Vertical and East-West accelerometers were deployed to reach this goal; and
- Force in the connection rods, especially for the PPDF connections.

Due to the large number of panels and connections compared to the number of sensors available, measurement locations were concentrated in the South-East corner of the building, as this was considered the most flexible. In addition to the analog sensors, four video cameras were installed to monitor the behavior of the panels during the FB testing: these recorded the behavior of the two types of corner joints, namely a PPDF connection and a flexing rod connection.

3.5 Physical inspections

Interior inspection of the cladding panels and connections was performed after each test (except for the first BI motions). In addition, exterior inspections, as time allowed, were per-

formed to evaluate the state of crack patterns on the panels as well as condition of the sealant between the panels. Upon observation of permanent displacement of a rod, selected connection rods were replaced between earthquake events. In addition, a complete replacement of the rods in the IP panels was performed prior to FB-4: ICA100, as the impending motion FB-5: DEN67 was intended to serve as the design earthquake event.

4 GLOBAL BUILDING RESPONSE

Figure 9 shows the peak floor accelerations (PFA) and peak interstory drift ratios (PIDR) of the building at its fifth and fourth floor. It is noted that accelerations were measured at every corner of each floor of the building, and displacements were obtained by double integration of these accelerations. The peaks in Figure 9 are the average of the maximum values of each of the four corners. As can be seen from Figure 9, the values of the PIDR and PFA were quite small for all BI tests, with the PIDR no greater than 0.15% at the 4-5th floor and the peak acceleration no greater than 0.23g on the fifth floor, during motion BI-7: ICA140. The first two FB motions, which were scaled to achieve serviceability demands within the building, reported peak accelerations and interstory drift ratios only slightly larger then those obtained in the final BI motion. The maximum value of PFA was obtained during motion FB-5: DEN67, when the structure observes considerable plastic deformation. The PFA at fifth floor was 0.68g, while 0.99g was measured at the roof slab. The largest PIDRs obtained on levels 4-5 and 5-roof were observed during the final motion FB-6: DEN100, with 1.2% and 0.8% attained on levels 4-5 and 5-roof, respectively. These values were lower anticipated, as soft story mechanism developed in the lower levels of the building, with very large PIDRs approaching 6% for the first two floors [14].

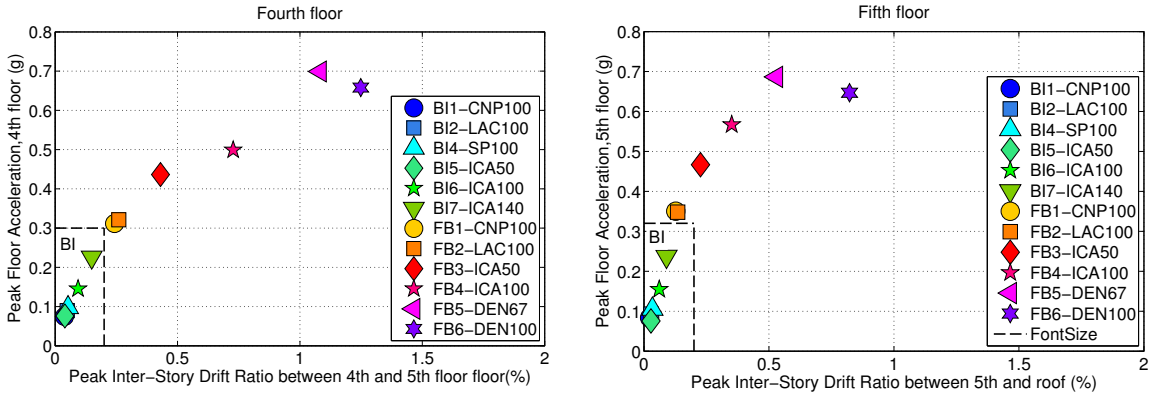

(a) (b)

Figure 9: Peak interstory drift ratio versus peak floor acceleration: (a) fourth floor, (b) fifth floor

5 DEVELOPMENT OF DAMAGE IN THE IP PANEL CONNECTIONS

Physical observations determined that, where it occurred, the damage to connections between the IP panels and building both for sliding rod and flexing rod connections, manifested primarily as a permanent bending of the rods. Even so, none of the rods actually fractured. This is likely due to a combination of ductile steel rod materials, bending mechanisms in the welded angle support clips, and the drifts imposed which were less than 1.5% (Figure 9). In what follows, the damage level will be indicated with the estimated lateral plastic distortion and angle of permanent bending of the rods.

5.1 Sliding rod connections

The sliding connections with snug rod (SRS) behaved well, as rod bending is virtually eliminated when the rod is snug to its connecting plate. Short rods within a sliding connection manifested no visible damage. These observations were confirmed during removal of the panels. In contrast, medium rod length sliding connections (SRM) developed plastic yielding during progressively increasing interstory drift demands, potentially due to abutting of the rod against the slotted plate or binding of the connection. Table 3 summarizes the physical observations, including noting when the rods were replaced during the motion sequence for the SRM at the 5th floor. The first notable damage to these connections was observed following motion FB-1. The plastic bend of the connection was barely visible and it was measured after the rod was removed. Subsequently, no additional visible damage to the SRM connections was noted until motion FB4-ICA100, during which one of the rods was severely permanently bent (25mm of residual drift in the connection, forming a 27° angle with the straight direction) as can be seen in Figure 10. The PIDR during this motion was only 0.35%. Interestingly, the residual deformation of the rod of 25mm was greater than the PID of 15mm, suggesting that the connection accumulated drift deformations through a ratcheting mechanism as the connection cycled back and forth, binding in one direction, while sliding in the other. This connection was replaced and was not damaged further, despite the much larger PIDR in subsequent motions.

Test	PID(PIDR) 5th floor-roof	Panel 5SW		Panel 5NW	
		Connection CW [Residual Deformation]	Connection CE [Residual Deformation]	Connection CW [Residual Deformation]	Connection CE [Residual Deformation]
BI	4mm(0.09%)	OK	OK	OK	OK
FB1	5mm(0.13%)	2mm *Replaced*	OK	OK	OK
FB2	6mm(0.14%)	OK	OK	OK	OK
FB3	10mm(0.23%)	OK *Replaced*	OK *Replaced*	OK *Replaced*	OK *Replaced*
FB4	15mm(0.35%)	25mm/27° *Replaced*	OK	OK	OK
FB5	23mm(0.53%)	OK	OK	OK	OK
FB6	35mm(0.82%)	OK	OK	OK	OK

Table 3: Progression of damage to SRM connections

Table 4 presents the progression of damage for the sliding connection with long rods (SRL) and their associated times of replacement. Similarly, these connections were not damaged during the BI tests, however, significant permanent deformation was observed during the FB motion sequence. In particular during FB-2:LAC100, when a PIDR of only 0.2% was reached, three of four connections were observed with permanent bends during post-event inspection. As it was clear that this configuration was not optimal, during replacement of these rods, the outside nut was not reinstalled to allow the rod to only carry tension, and to alleviate binding from clamping of the plate washers during rotation. This new configuration performed reasonably well during motion FB-4: ICA100 (with only one connection slightly damaged). During motions FB-5 and FB-6 (PIDR=1.2%), however, these connections were severely

plastically bent again, demonstrating the difficulty of utilizing a very long rod for this type of connection. Examples of the physical damage to the SRL connections are shown in Figure 10.

Test	PID(PIDR) 4^{th}-5^{th} floor	Damage to panel 4SW		Damage to panel 4NW	
		Connection CW [Residual Deformation]	Connection CE [Residual Deformation]	Connection CW [Residual Deformation]	Connection CE [Residual Deformation]
BI	6mm(0.15%)	OK	OK	OK	OK
FB1	10mm(0.24%)	25mm (14°) *Replaced*	OK	OK	OK
FB2	11mm(0.26%)	25mm (14°)	25mm (14°)	OK	30mm (17°)
FB3	18mm(0.43%)	55mm (30°) *Replaced (no nut)*	50mm (27°) *Replaced (no nut)*	OK *Replaced (no nut)*	60mm (32°) *Replaced (no nut)*
FB4	31mm(0.72%)	OK	OK	10mm (<1°)	OK
FB5	47mm(1.11%)	OK	25mm (14°)	0mm	OK
FB6	53mm(1.24%)	OK	60mm (32°)	5mm (<1°)	25mm (14°)

Table 4: Progression of damage to SRL connections

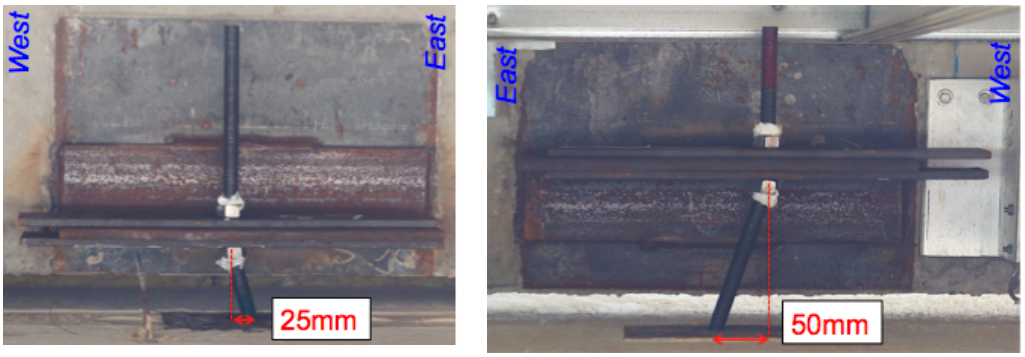

(a) (b)

Figure 10: Example of damage to sliding rod connections. (a) SRM type, connection CW/panel SW after FB4-ICA100 and (b) SRL type, connection CE/Panel 4SW after FB3-ICA50.

5.2 Flexing rod connections

Similarly, a synthesis of visible damage to the flexing rod connection is presented in Tables 5 and 6, with example photographs shown in Figure 11. Damage was manifested via plastic hinging of the rod at the nut location (Figure 11). Residual damage to the flexing rod connections with short rods was not detected. It should be noted that inspection of these connections was possible only on the fifth floor, noting that this level attained smaller PIDRs. The flexing rod connections with a medium length rod (FRM) on the fourth floor were permanently bent during motions FB5 and FB6 at the fourth floor while only during FB6 did they plastically yield at the fifth floor (Table 5). Flexing rod connections with long rods (FRL) exhibited residual damage only after motion FB6, and only at the panel on the fourth floor (Table 6).

Test	PID(PIDR) 4-5th floor	Damage to panel 4NE Connection WW [Residual Defor-mation]	Connection EE [Residual Defor-mation]	PID(PIDR) 5thfloor-roof	Damage to panel 5NE Connection WW [Residual Defor-mation]	Connection EE [Residual Defor-mation]
BI	6mm(0.15%)	OK	OK	4mm(0.09%)	OK	OK
FB1	10mm(0.24%)	OK	OK	5mm(0.13%)	OK	OK
FB2	11mm(0.26%)	OK	OK	6mm(0.14%)	OK	OK
FB3	18mm(0.43%)	OK *Replaced*	OK *Replaced*	10m(0.23%)	OK *Replaced*	OK *Replaced*
FB4	31mm(0.72%)	OK	OK	15mm(0.35%)	OK	OK
FB5	47mm(1.11%)	30mm (4°)	45mm (6°)	23mm(0.53%)	OK	OK
FB6	53mm(1.24%)	20mm (3°)	40mm (6°)	35mm(0.82%)	OK	25mm (3°)

Table 5: Progression of damage to the connection FRM

Test	PID/PIDR 4th-5th floor	Damage to panel 4NE Connection CW [Amount of bent]	Connection CE [Amount of bent]
BI	6mm(0.15%)	OK	OK
FB1	10mm(0.24%)	OK	OK
FB2	11mm(0.26%)	OK	OK
FB3	18mm(0.43%)	OK *Replaced*	OK *Replaced*
FB4	31mm(0.72%)	OK	OK
FB5	47mm(1.11%)	OK	OK
FB6	53mm(1.24%)	40mm (4°)	OK

Table 6: Progression of damage to the connection FRL

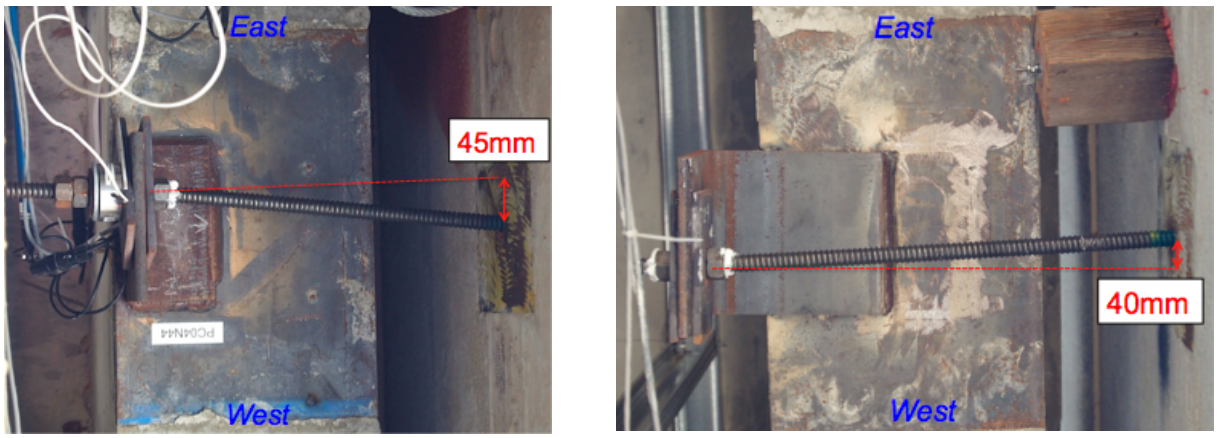

(a) (b)

Figure 11: Damage to flexing rod connections: (a) FRM type, connection EE in panel 4NE after FB5-DEN67, (b) FRL type, connection CW in panel 5NE after FB6-DEN100

6 IN-PLANE DISPLACEMENT OF THE IP PANELS

In each of the eight IP panels, the in-plane displacement absorbed by the push pull connections at the top of the panels (Δ_c^{panel}) was measured. Moreover, it was possible to find the theoretical ID at the centerline of the panels assuming a weighted average of the ID measured at the corners of the building (ID^{panel}). From these measurements, it is clear that the behavior of panels with sliding rod connections and flexing rod connections was quite different. Figure 12 shows a view of the time history of Δ_c^{panel} and ID^{panel} for the panels on the South Side for the fourth floor of the building (4SW, utilizing sliding rod connections, and 4SE, utilizing flexing rod connections) for three different motions. During the final BI motion (BI-7:ICA140, Figure 12a and 12b) Δ_c^{panel} was smaller than ID^{panel} for both panels. However, while at the panel with sliding connections Δ_c^{panel} was quite similar to ID^{panel}, in the panel with flexing rod connections Δ_c^{panel} was half of the total ID^{panel} ,meaning that in this panel half of the drift was absorbed by a deformation of the panel itself.

The behavior changed during FB phase of testing. Figure 12c and 12d show that, even for the small FB-1:CNP100 record, Δ_c^{panel} was slightly larger than ID^{panel} for the panel with sliding connections, while it still was smaller that the ID^{panel} for the panel with flexing rod connections. The behavior of the sliding connection can be understood considering the force-displacement behavior of a frictional system: once the value of the force reaches the force necessary to activate the motion (F_M), the sliding is activated and the displacement can increase without increment in force until the force goes back to be less that F_M and the mechanism locks. The behavior is of course different when the movement is controlled by bending of the steel such as occurs in the flexing rod connections. In this case, resistance of the steel can limit the displacement, especially if the steel is elastic or only slightly plastic. It should be noted that, since the panels were installed at the upper floors, acceleration (and consequently forces), reached considerable values. This behavior observed in FB-1:CNP100 continued up to FB-4:ICA100 with the difference between Δ_c^{panel} and ID^{panel} increasing for the panel with sliding rod connections and decreasing for panel with flexing rod connections. During the last two motions, the amplitude of Δ_c^{panel} for the panel with flexing rod connections approaches the ID^{panel}. Figure 12e and 12f show an asymmetric behavior of the panel with flexing rod connections, namely, Δ_c^{panel} was larger than ID^{panel} for the movement in the positive direction (Eastward), while it was still smaller than the ID^{panel} for movements in the negative direction (Westward). The asymmetry in the behavior might be due to some permanent deformation of the flexing rod (as observed in the inspection phases), which initiated exactly during the design motion FB-5:DEN67.

Scatter plots summarizing the peaks of the ID^{panel} versus the peak Δ_c^{panel} for each motion are presented in Figure 13. Results for the panels at the fourth floor (respectively moving in the Eastward/positive direction and in the Westward/negative direction) are presented in Figure 13a and Figure 13b. As already observed from the time histories, the displacement Δ_c^{panel} was always smaller than ID^{panel} during the BI motions. In addition, the panels with sliding rod connections had a Δ_c^{panel} greater than the ID^{panel} for all of the FB motions. It can be seen also that the increment of Δ_c^{panel} with respect to the ID^{panel} followed a specific trend, and that this trend is more pronounced in the Eastward direction than in the Westward direction. The displacement of the panels with flexing rod connections is asymmetric, namely, in the Eastward direction it follows a trend incrementally similar to that of the sliding rod connections, while in the Westward direction the displacement is mostly smaller than the ID^{panel}, though it approaches a 1:1 line during the last motion. The behavior of the panels on the fifth floor can be seen in Figure 13c (Eastward movement) and Figure 13d (Westward movement). The behavior of the panels with sliding rod connections in the Eastward direction is similar to that ob-

served on the fourth floor. For the Westward movement Δ_c^{panel} is initially smaller than ID^{panel} and then it keeps really similar to it. In this case, the panels with flexing rod connections show a Δ_c^{panel} smaller the ID^{panel} for all the cases.

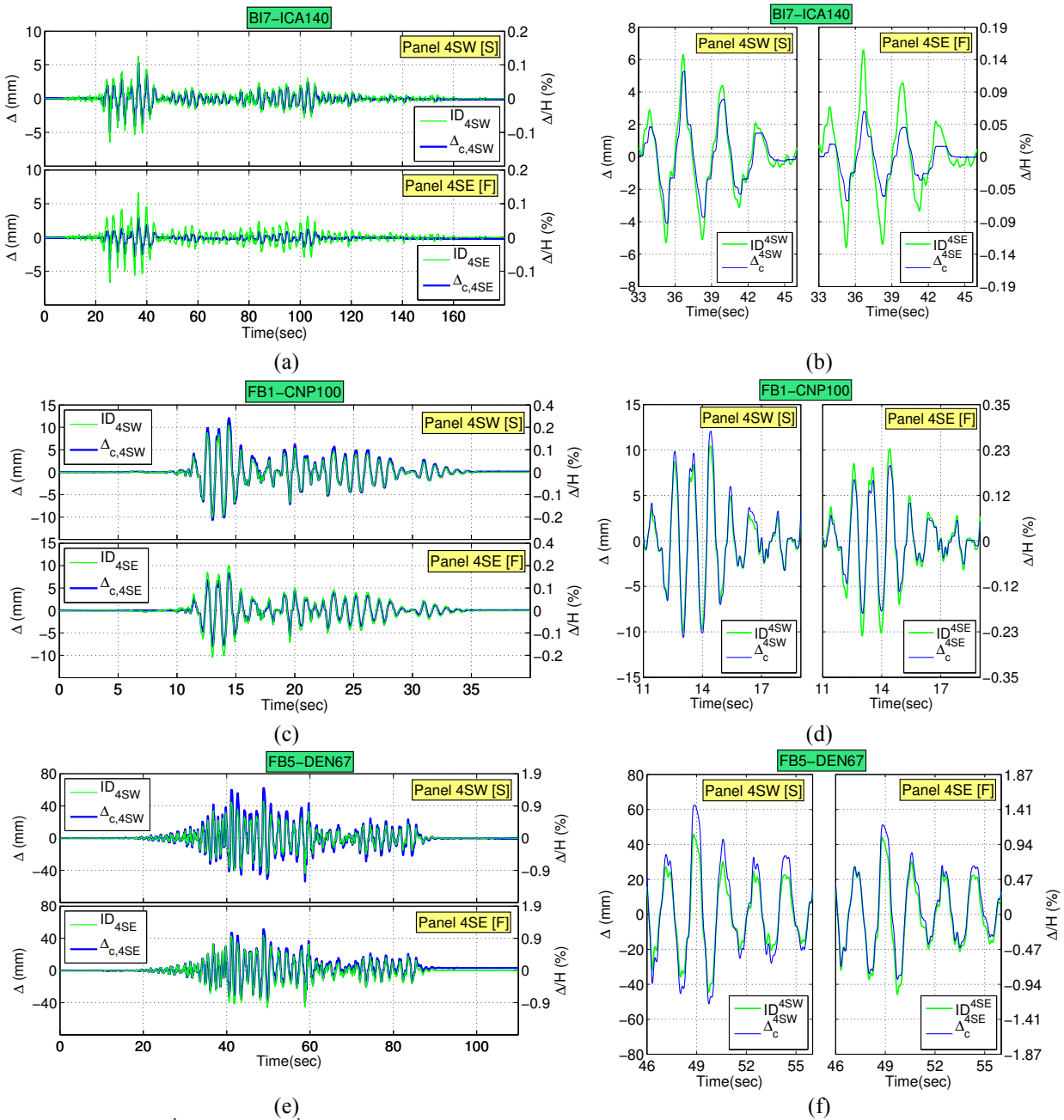

Figure 12: ID^{panel} versus Δ_c^{panel} for panel 4SW(sliding connections) and 4SE(flexing rod connections). (a) BI7-ICA140, (b) FB1-CNP100, (c) FB4-ICA100, (d) FB5-DEN67.

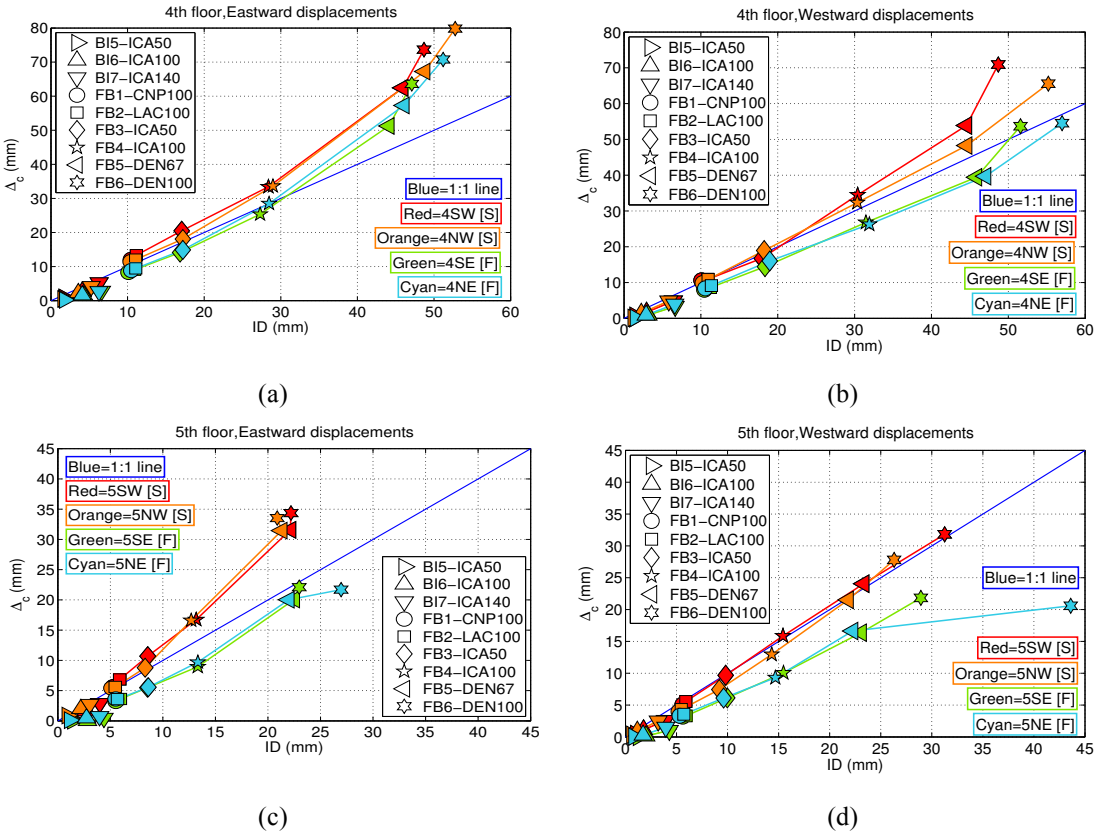

Figure 13: Peak ID versus peak Δ_c : (a) Panels on the fourth floor-Eastward displacement, (b) Panels on the fourth floor-Westward displacement, (c)Panels on the fifth floor-Eastward displacement, (d) Panels on the fifth floor-Westward displacement.

7 CONCLUSIONS

Sixteen precast concrete cladding panels were installed on the upper two floors of a five-story building and subjected to a series of earthquake motions, first with the building in a base-isolated configuration, and then in a fixed-base configuration (BI and FB test phases, respectively). Two types of push-pull connections were tested and their ability to accommodate in-plane story drifts assessed. Namely, flexing rod and sliding rod connections of varying rod lengths were installed and tested in an effort to understand the relationship between rod length and connection performance. Inspection of residual damage after each test motion revealed that the connections did not undergo any substantial damage during the BI motions. During the FB tests however, plastic yielding of both the flexing rod and sliding rod connections were observed, with the exception of the sliding short rod connections, which showed no signs of damage under any test. Sliding rods of a medium length showed minor plastic yielding in most of the tests. Flexing rod connections behaved better, with no residual damage observed in the flexing rod connections with short rods, and plastic yielding observed during the design and maximum credible scaled earthquake motions FB5 and FB6 (PIDR as low as 0.8%), while the one with the long rod was damaged only during FB6 (PIDR 0f 1.2%).

Displacement absorbed by the connection (Δ_c) was compared with the interstory drift (ID) for all of the IP panels. It was found that panels with sliding rod and flexing rod connection behaved in vastly different ways, especially while the building was fixed at its base. During these tests, for the panels with sliding rod connections, the connection displacement Δ_c was greater than the ID because of the frictional behavior of the connections, while for the panels with flexing rod connections Δ_c was smaller than the ID up to FB-4.

A new concept connection was also tested – where the building corner joints were intentionally undersized – forcing a collision of out-of-plane tilting panels with in-plane translating panels around the corner. The push-pull connection accommodated the panel collision through the development of a plastic ductile fuse that limited the force on the connection fasteners and anchorages.

Data from these experiments will lay the foundation for contributing to design guidelines specific to precast concrete cladding, with a focus on defining acceptable behavior of connections and panel joints. The current practice in the U.S. is governed by the requirements of ASCE 7, Section 13.5.3, which provides qualitative performance guidelines for panel joints and connection ductility. The design guidelines supported by this testing will provide a quantitative approach to the existing state of the practice.

ACKNOWLEDGEMENTS

This project is a collaboration between four academic institutions (University of California, San Diego, San Diego State University, Howard University, and Worcester Polytechnic Institute), four government or other granting agencies (the National Science Foundation, the Englekirk Advisory Board, the Charles Pankow Foundation, and the California Seismic Safety Commission), over 40 industry partners, and two oversight committees. A listing of industry project sponsors may be found on the project website: http://bncs.ucsd.edu/index.html. Through the NSF-NEESR program, partial funding is provided by grant number CMMI-0936505, where Dr. Joy Pauschke is the program manager. The above continuous support is gratefully acknowledged. Many individuals contributed to the overall effort of this project. However, we specifically thank core team members Profs. Jose Restrepo and Joel Conte, doctoral students Rodrigo Astroza, Hamed Ebrahimian, Steven Mintz, and Xiang Wang, the NEES@UCSD and NEES@UCLA staff, Mr. Robert Bachman, Dr. Robert Englekirk, Mr. Mahmoud Faghihi, Dr. Matthew Hoehler of Hilti Corp., Prof. Ken Walsh of SDSU, and SDSU students Consuelo Aranda and Elias Espino. Specific to the PCC effort described in this paper, the authors thank the PCI and its R&D Council members, the Charles Pankow Foundation, Clark-Pacific, and Willis Construction, and Regal Industries and specifically Roger Becker and Prof Kurt McMullin for their collaboration and continued support. Opinions, findings, and conclusions expressed are those of the authors, and do not necessarily reflect those of the sponsoring organization.

8 REFERENCES

[1] E. Miranda, G. Mosqueda, R. Retamales, G. Pekcan, Performance of Nonstructural Components during the 27 February 2010 Chile Earthquake. *Earthquake Spectra*, 28(S1), S453–S471, June 2012.

[2] S. Taghavi, E. Miranda, Response Assessment of Nonstructural Building Elements, *Technical Report PEER 2003/05*, Pacific Earthquake Engineering Research Center, University of California, Berkeley.

[3] A. Baird, A. Palermo and S. Pampanin, Façade damage assessment of multi-storey buildings in the 2011 Christchurch earthquake, Bullettin of the New Zealand Society for Earthquake Engineering, **44/4**, 368-376, December 2011.

[4] Iverson, J.K., Hawkins, N.M., "Performance of Precast/Prestressed Concrete Building Structures During Northridge Earthquake" PCI Journal March/April 1994

[5] S. K. Ghosh, N. M. Cleland, Performance of Precast Concrete Building Structures. Earthquake Spectra, **28S1**, S349–S384, June 2012.

[6] Miyamoto International, L'Aquila, Italy, Earthquake Field Investigation Report, West Sacramento, CA, 2009.

[7] K.M. McMullin, M. Ortiz, L. Patel, S. Yarra, T. Kishimoto, C. Stewart and B. Steed, Response of Exterior Precast Concrete Cladding Panels in NEES-TIPS/NEES-GC/E-Defense Tests on a Full Scale 5-story Building. *Structures Congress 2012* (ASCE 2012), Chicago, Illinois, March 29-31 2012.

[8] A. Barid, A. Palermo, S. Pampanin, Experimental and numerical validation of seismic interaction between cladding systems and moment resisting frames. 15th World Conference on Earthquake Engineering (15 WCEE 2012), Lisbon, Portugal, September 24-28, 2012.

[9] American Society of Civil Engineers, ASCE 7-10 Minimum Design Loads for Buildings and Other Structures, ASCE.

[10] American Concrete Institute Committee 318, 318-08: Building Code Requirements for Structural Concrete and Commentary, ACI 2008.

[11] Precast/Prestressed Concrete Institute, PCI MNL-120-0, PCI Design Handbook-Precast and Prestressed Concrete, 6th Edition, 2004.

[12] American Institute of Steel Construction, Specification for Structural Steel Buildings ANSI/AISC 360-05, AISC,2005.

[13] Wang, X., Ebrahimian, H., Astroza, R., Conte, J., Restrepo, J. and Hutchinson, T. (2013). "Shake table testing of a full-scale five-story building: pre-test simulation of the test building and development of a nonstructural components and systems design criteria," Proceedings, *ASCE Structures Congress*, ASCE, Pittsburgh, PA, May 2013.

[14] T. Hutchinson, J. Restrepo, J. Conte, B. Meacham, Overview of the Building Nonstructural Components and Systems (BNCS) project. *Proceedings, ASCE Structures Congress*, ASCE, Pittsburgh, PA, May 2013.